Dynamic Nuclear Polarization and the Paradox of Quantum Thermalization

Andrea De Luca and Alberto Rosso
Laboratoire de Physique Théorique et Modèles Statistiques (UMR CNRS 8626), Université Paris-Sud, Bât. 100, 15 rue Georges Clémenceau, 91405 Orsay Cedex, France
(Received 20 May 2015; published 20 August 2015)

Dynamic nuclear polarization (DNP) is to date the most effective technique to increase the nuclear polarization opening disruptive perspectives for medical applications. In a DNP setting, the interacting spin system is quasi-isolated and brought out of equilibrium by microwave irradiation. Here we show that the resulting stationary state strongly depends on the ergodicity properties of the spin many-body eigenstates. In particular, the dipolar interactions compete with the disorder induced by local magnetic fields resulting in two distinct dynamical phases: while for weak interaction, only a small enhancement of polarization is observed, for strong interactions the spins collectively equilibrate to an extremely low effective temperature that boosts DNP efficiency. We argue that these two phases are intimately related to the problem of thermalization in closed quantum systems where a many-body localization transition can occur varying the strength of the interactions.

DOI: 10.1103/PhysRevLett.115.080401 PACS numbers: 05.30.-d, 72.15.Rn, 75.10.Nr, 76.60.-k

Introduction.—Formulating statistical mechanics for an isolated many-body system requires the tacit assumption of ergodicity. Only recently, however, the eigenstate thermalization hypothesis (ETH) [1,2] promoted this concept to a testable condition at the quantum level, allowing the identification of situations where ergodicity might even be broken once disorder combines with quantum interference [3,4]. It is natural to ask, then, whether ETH influences also the stationary regimes where energy is constantly injected and dissipated, leading again to an emergent simple description. Dynamic nuclear polarization (DNP), the most effective technique to increase the nuclear polarization, is a paradigmatic out-of-equilibrium protocol to test these ideas. In a DNP procedure [5], the compound is doped with radicals (i.e., molecules with unpaired electrons), exposed to a strong magnetic field at low temperature β^{-1} and then irradiated with microwaves (see Fig. 1 for details). At thermal equilibrium, the unpaired electrons are much more polarized than nuclear spins because the electron Zeeman gap is orders of magnitude larger than the nuclear one. When the microwaves are on, at a frequency close to the electron Zeeman gap, the spin system of interacting electrons and nuclei organizes in an out-of-equilibrium steady state with a huge nuclear polarization. The hyperpolarized sample can then be dissolved at room temperature [6], injected in patients, and used as a metabolic tracer [7]. However, our understanding of the physical mechanisms that trigger hyperpolarization is still poor. A striking experimental evidence is the thermal mixing of the ensemble of different nuclear spins (^{13}C, ^{15}N, ^{89}Y, …) [8,9]: their enhanced polarizations are well described by an equilibriumlike polarization, $P_n = \tanh(\beta_s \hbar \omega_n/2)$ (see Fig. 1, right). While the Zeeman gap ω_n depends on the nuclear species, the spin temperature β_s^{-1} is a unique parameter, possibly one thousand times smaller than β^{-1}, the one of the bath [10].

But how can a quantum system appear thermal and colder when irradiated by microwaves? In which way can the spin temperature be controlled acting on the experimental parameters?

In this Letter we show that the spin temperature concept is directly connected to quantum ergodicity and ETH. While for classical physics thermalization has its origin at the onset of chaotic dynamics, quantum ergodicity requires the ETH, a thermal behavior at the level of single eigenfunctions [1,11]. The realm of ETH is normally restricted to quench protocols in cold atom experiments,

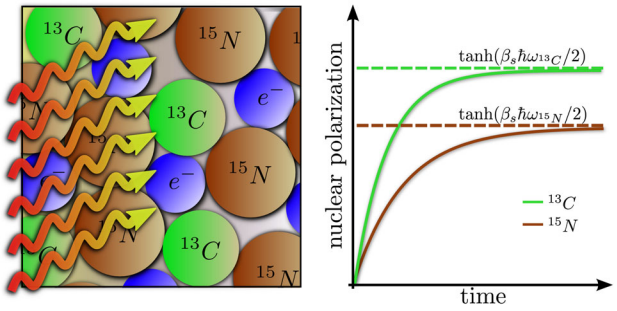

FIG. 1 (color online). A solid material containing nuclear spins (e.g., ^{13}C, ^{15}N) and doped with molecules with unpaired electrons (left). At 1.2 K and 3.35 T the equilibrium polarization of the electron spins is very high, (94%), while nuclear spins are very little polarized, less than 1%. Under microwave irradiation the spin system evolves towards a new steady state characterized by a single spin temperature $\beta_s^{-1} \sim 1$ mK (right). In this work, we analyze exclusively the electron spins and show that an out-of-equilibrium spin temperature results from the interplay of disorder and interaction.

where any exchange of energy with the environment is under control. Our work shows that ETH may impose a thermal behavior to the stationary state of open quantum systems, giving a practical and experimental relevance to the fundamental problem of quantum thermalization [3,4].

The microscopic model.—The traditional description of DNP in the thermal mixing regime relies on the phenomenological assumption that the electron spins cool down once irradiated and act as a reservoir for all nuclear species. Here, we focus only on the electron spins and on the origin of the spin temperature in their stationary state. In the electron spin Hamintonian, the presence of g-factor anisotropy induces a spread of the electron Zeeman gap:

$$\hat{H} = \hbar \sum_{i=1}^{N} (\omega_e + \Delta_i)\hat{S}_z^i + \hat{H}_{\rm dip}, \tag{1}$$

where N is the number of electrons and ω_e is the external magnetic field. The random fields Δ_i are quenched at low temperature and distributed according to the density $f(\Delta)$, with mean $\overline{\Delta_i} = 0$ and variance $\overline{\Delta_i^2} = \Delta\omega_e^2$. The term $\hat{H}_{\rm dip}$ contains the interactions between spins due to the dipolar coupling. Experiments can access the product $f(\Delta)P_e(\omega)$, dubbed EPR spectrum, where $P_e(\omega)$ is the polarization of an electron with Zeeman gap $\omega = \omega_e + \Delta_i$. At equilibrium with the environment (sketched in blue in Fig. 2), $P_e(\omega) \simeq -1$. The microwave irradiations at frequency $\omega_{\rm MW}$ and intensity ω_1 take the form $\hat{H}_{\rm MW} = 2\omega_1 \hat{S}_x \cos(\omega_{\rm MW} t)$, with $\hat{S}_x$ the total spin operator along the x component. In the absence of dipolar interactions, the Bloch equations predict that the electrons with a resonating Zeeman gap are saturated, $P_e(\omega \sim \omega_{\rm MW}) \sim 0$, while the others remain highly polarized. This corresponds to the *hole burning shape* of the EPR spectrum, shown in Fig. 2(a). On the contrary, according to the thermal mixing picture, the presence of dipolar interactions induces a collective reorganization of the electron polarization profile $P_e(\omega)$, that shows an equilibriumlike shape even under microwave irradiation

$$P_e(\omega) = -\tanh\left[\frac{\hbar\beta_{\rm s}}{2}(\omega - \omega_0)\right] \tag{2}$$

with $\omega_0 \simeq \omega_{\rm MW}$. The ansatz of Eq. (2) lacks a microscopic derivation. Moreover, recent *ab initio* models [12] have only observed a hole burning shape, with a weak polarization enhancement triggered by local hybridizations [13–15]. Here, we take

$$\hat{H}_{\rm dip} = \sum_{i<j} A_{ij}(\hat{S}_+^i \hat{S}_-^i + \text{c.c.}). \tag{3}$$

where the $A_{i,j}$ are the dipolar couplings. Because of the glassiness of DNP samples, the distance between electrons is random and, thus, for simplicity the coupling A_{ij} are taken, within a mean field approximation, as Gaussian random variables with zero mean and variance U^2/N. We are interested in the strongly correlated regime where disorder and interaction compete, i.e., $U \simeq \Delta\omega_e$. Our conclusions should not depend on the specific model and, here, we choose a uniform distribution of local magnetic fields by taking equally spaced $\Delta_i = \Delta\omega_e(2i - N - 1/2N)$, with randomness only affecting the dipolar couplings.

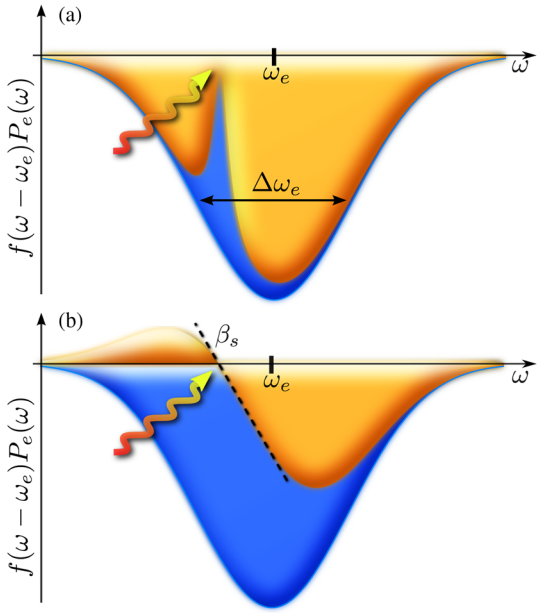

FIG. 2 (color online). EPR spectrum. Equilibrium (blue) versus MW irradiated (yellow) profile. Under irradiation two possible profiles are expected: (a) The hole burning shape, characteristic of the noninteracting case; (b) the hyperbolic tangent shape characterized by a very low effective temperature β_s that cools down the nuclear spins.

The master equation.—A key experimental observation [16,17] is that the spin system is quasi-isolated with a dephasing time T_2, very short compared to the time scales of microwave dynamics and to the relaxation time T_1, with the thermal bath [18]. Therefore, any initial density matrix ρ is quickly reduced by dephasing to a diagonal form in the basis of eigenstates of $\hat{H}$. In practice [19], the Lindblad equation $\dot{\rho} = \mathcal{L}\rho$ used to describe the dynamics of the open system reduces to a master equation for the time evolution of the 2^N occupation probabilities, ρ_{nn} with rates $W_{n\to n'} = h(\Delta\epsilon_{n,n'})W_{n,n'}^{\rm bath} + W_{n,n'}^{\rm MW}$, where

$$W_{n,n'}^{\rm bath} = \frac{2}{T_1}\sum_{j=1}^{N}\sum_{\alpha=x,y,z} |\langle n|\hat{S}_\alpha^j|n'\rangle|^2, \tag{4a}$$

$$W_{n,n'}^{\rm MW} = \frac{4\omega_1^2 T_2 |\langle n|\hat{S}_x|n'\rangle|^2}{1 + T_2^2(|\Delta\epsilon_{nn'}| - \omega_{\rm MW})^2}. \tag{4b}$$

Here the index n labels eigenstates of energy ϵ_n with $\Delta\epsilon_{nn'} = \epsilon_n - \epsilon_{n'}$. The function $h(x) = e^{\beta x}/(1 + e^{\beta x})$

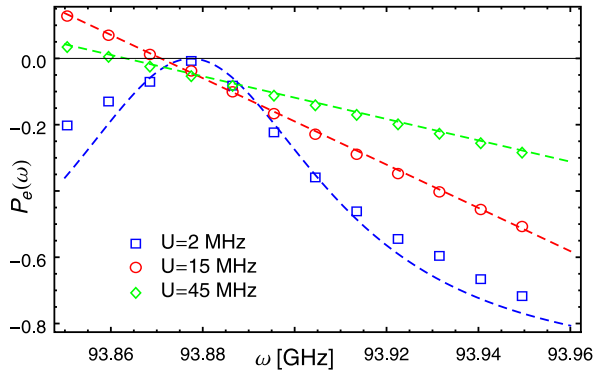

FIG. 3 (color online). Electron polarization under MW irradiation with $\omega_{\mathrm{MW}} = 93.8775$ GHz, for the model of Eq. (1) with $N = 12$ spins. For strong dipolar interactions (circles and diamonds) the spin temperature is well defined. The fit according to Eq. (2) (red and green lines) gives $\beta_s^{-1} = 3.7$ mK for $U = 15$ MHz and $\beta_s^{-1} = 7.4$ mK for $U = 45$ MHz. For weak interactions $U = 2$ MHz (square) a simple broadening of the hole burning noninteracting profile (dashed blue line) given in Eq. (8) of Ref. [19].

assures the convergence to Gibbs equilibrium when the microwaves are off and the rate $W^{\mathrm{bath}}_{n,n'}$ in Eq. (4a) comes from single spin flip transitions on a time scale T_1. Equation (4b) describes transitions induced by the microwave field. In Fig. 3 we present the stationary value of the polarization $P_e(\omega = \omega_e + \Delta_i) \equiv 2\mathrm{Tr}[\hat{S}^i_z \rho_\infty]$, computed from the stationary occupation probabilities which solve $\mathcal{L}\rho_\infty = 0$. Note that this requires the full diagonalization of $\hat{H}$, strongly constraining the possible system sizes.

Two possible behaviors are observed: For weak interactions, the hole burning shape, already observed in Refs. [13–15], is recovered. Instead, in the presence of strong dipolar interactions, we show that all electrons rearrange according to the spin temperature profile of Eq. (2). Remarkably, in the wing closer to ω_{MW}, electron polarization can even invert its sign.

The origin of these two dynamical regimes can be understood in relation with the quantum thermalization of the electron spins. In general, in closed quantum systems, an arbitrary initial state converges to a time-independent density matrix because of dephasing: in the basis of eigenstates, off-diagonal elements are suppressed while the occupation probabilities on the diagonal remain constant. But then, how could thermodynamics emerge if the initial occupancies are conserved? In Fig. 4 (left) we report the most probable value of the local polarization for the eigenstates at a given energy. In presence of weak interaction ($U = 2$ MHz) the polarization fluctuates between the extremal values ± 1 showing that the exact eigenstates are almost factorized on local spins. When the interaction is increased, eigenstates are strongly entangled and the local polarization is close to zero, its microcanonical average. As predicted by ETH, each eigenstate is independently thermal and so the paradox of quantum thermalization is solved, as the memory of the initial condition fades out while entanglement grows through dephasing [24]. Instead, in the weakly interacting regime, for initial states close enough to exact eigenstates, a finite fraction of the polarization is doomed to survive [25–27].

In absence of disorder, the spin temperature is well defined but very high [28]; varying the ratio $U/\Delta\omega_e$, the spin temperature decreases up to a point where the system approaches the many-body localization (MBL), a dynamical transition between an ETH and a non-ergodic phase [3,4,29], surviving even in the presence of microwaves [30]. In Fig. 4 (middle) we present a standard indicator for the transition: the variation of the local polarization between pairs of adjacent eigenstates versus the size of the system [4]. In the ETH phase, this quantity converges exponentially to zero, indicating that all the fluctuations are

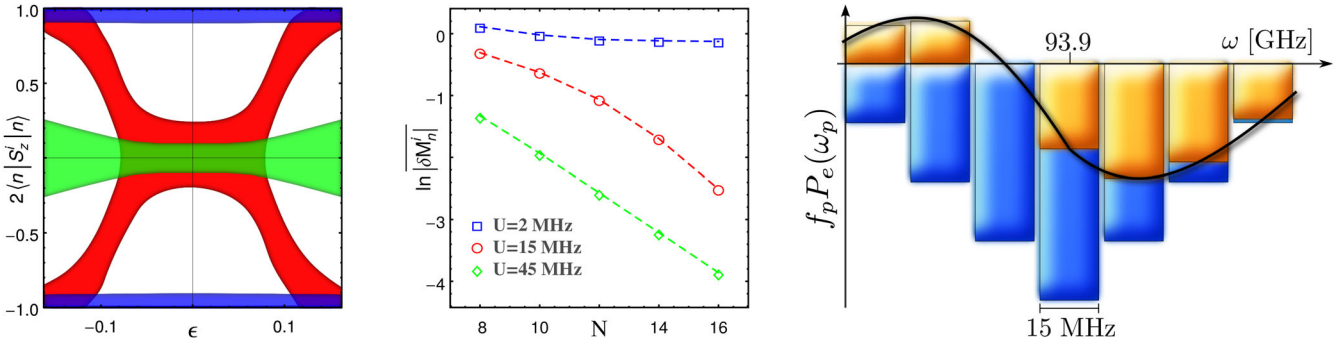

FIG. 4 (color online). Left: Density plot of the distribution of diagonal elements $\langle n|\hat{S}^i_z|n\rangle$ in the sector of vanishing total polarization. Colored regions represent, for each energy window $(\epsilon, \epsilon + \Delta\epsilon)$, the smallest area containing half probability ($U = 2$ MHz in blue, $U = 15$ MHz in red, $U = 45$ MHz in green). Middle: Logarithm of the variation of the local polarization between pairs of adjacent eigenstates of Eq. (1) versus N. In the ergodic phase, this indicator vanishes exponentially in N. In the localized phase, it saturates to a finite value. Right: EPR spectrum for the toy model of Eq. (5) with 7 packets. The equilibrium profile is in blue. The yellow histograms show the stationary profile under MW irradiation with $\omega_{\mathrm{MW}} = 93.8775$ GHz, $N = 64$ spins and $f_p = N_p/N$. The solid line is obtained from the ansatz of Eq. (2) imposing the condition (6).

more and more suppressed. On the contrary, in the localized phase, it saturates to a finite value, since fluctuations remain present even in the thermodynamic limit.

Our results indicate that whenever the interaction with the environment is weak but not negligible, the dynamics reduces to quantum jumps between exact eigenstates of the electron system. Then, if ETH holds, the stationary state necessarily looks thermal, with few global parameters (e.g., the spin temperature), fixed relaxation, and microwave irradiation. Instead, in the localized phase, only a weak DNP enhancement, triggered by few-body processes, can be observed.

Spin temperature behavior.—It is important now to estimate the value of the spin temperature in the ETH phase. We first study a simplified model where the electrons in the EPR spectrum are assumed to be grouped into well separated macroscopic packets:

$$\hat{H}_{\mathrm{toy}} = \hbar \sum_{p} (\omega_e + \Delta_p) \sum_{k=1}^{N_p} \hat{S}_z^k + \eta \hat{H}_{\mathrm{int}}, \tag{5}$$

where $\sum_p N_p \Delta_p = 0$ and N_p is the number of electrons in the packet p. For $\eta = 0$ the spectrum of the Hamiltonian is composed by sectors of defined total magnetization and energy. The interactions are encoded in H_{int}, which is chosen as a Gaussian random matrix inside each sector. When η is small—but still prevailing over the coupling with the bath—H_{int} lifts the degeneracies in each sector selecting an ergodic basis in which the long-time density matrix is diagonal [31]. This model allows avoiding the numerical diagonalization, since statistical properties of the eigenstates are known. Moreover, the rates $W_{n\to n'}$ in Eq. (4) depend on n, n' only via the matrix elements of local spin operators, $|\langle n|\hat{S}_x^i|n'\rangle|^2$. Since the eigenvectors are perfectly ergodic in each sector, this quantity is actually determined by the pair of sectors containing, respectively, n, n', with weak statistical fluctuations [19]. These simplifications largely reduce the exponential difficulty of the problem. In Fig. 4 (right) we show that the stationary EPR spectrum for $N = 64$ spins perfectly agrees with the thermal ansatz in Eq. (2). Moreover, β_s and ω_0 in Eq. (2) can be fixed, imposing that the energy and total magnetization become stationary for large times, which for the toy model leads to [19]

$$2T_2\omega_1^2 P_e(\omega_{\mathrm{MW}}) + \sum_p N_p \frac{P_e(\omega_p) - P_0}{2T_1} = 0, \tag{6a}$$

$$2T_2\omega_1^2 \Delta_0 P_e(\omega_{\mathrm{MW}}) + \sum_p N_p \Delta_p \frac{P_e(\omega_p) - P_0}{2T_1} = 0, \tag{6b}$$

where $\omega_p = \omega_e + \Delta_p$, $P_0 = -\tanh(\beta\omega_e/2)$ is the equilibrium polarization, $\Delta_0 = \omega_e - \omega_{\mathrm{MW}}$ and we assumed that the microwaves only act on the resonating packet. Note that, for conserved quantities of Eq. (5), as the energy and the total magnetization, the balance of the flows has a simple form since it reduces to the exchanges with the bath and microwaves.

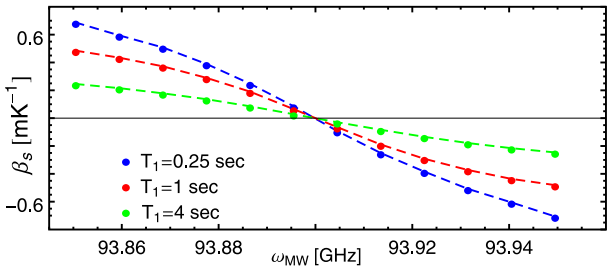

FIG. 5 (color online). T_1 shortening effect. The spin temperature β_s, obtained from the fit of the electron polarizations (see Fig. 3), is shown versus ω_{MW} with $U = 15$ MHz and different values of the relaxation time T_1: the spin temperature is smaller when relaxation is faster, consistently with the observed increase in the hyperpolarization efficiency [34,35].

These results retrace the traditional prediction obtained within the phenomenological ansatz of Eq. (2) proposed by Borghini [32]. Here, Eq. (2) naturally emerges once the strong suppression of fluctuations, characteristic of the ETH phase, has been assumed. However, the qualitative approach to hyperpolarization provided by this toy model largely underestimate the spin temperature value and hides its dependence from the microscopical parameters $(U, T_1, \ldots)$ [33].

A richer scenario emerges instead from the exact diagonalization of Eq. (1), where a stronger hyperpolarization enhancement is observed approaching the MBL transition (see Fig. 3) and can be even amplified decreasing the relaxation time T_1 (see Fig. 5). Both effects agree with two well-known experiments, which fall beyond the applicability of the Borghini model [36]. The first showed that the enhancement occurs only at relatively low radical concentrations [16], and therefore at weaker dipolar interactions. In the second, the addition of gadolinium complexes was used to induce a reduction of the relaxation time T_1 [34,35]. This, in turn, improved the signal enhancement and gadolinium is now commonly exploited in standard protocols for DNP sample preparation.

Concluding remarks.—We presented a simple model for the study of DNP, providing a realistic dependence on the tunable parameters. The concept of out-of-equilibrium spin temperature emerges naturally as a macroscopic manifestation of the ETH for the electron spin Hamiltonian.

Our study candidates DNP as a good ground for the direct observation of the MBL transition and its dynamical phase diagram. Two key advantages play in favor of this experimental setting. The first is that the two relevant control parameters for the transition are tunable: U depends on the radical concentration and $\Delta\omega_e$ is proportional to the external magnetic field. The second is that the system does

not require being isolated during the characteristic observation time, but, rather, that the relaxation is sufficiently slow to allow the pure quantum behavior to settle. Note that, in the past, the spin-temperature polarization profile was already experimentally observed in Ref. [37] for increasingly g factors anisotropy, up to a critical value where the hole-burning profile popped out. The possibility of performing experiments precisely aimed at the observation of the elusive critical regime of the MBL is therefore concrete and promising. Moreover, the tunability of external parameters may allow the exploration of the phase diagram, even in regimes where the physics of spin glasses becomes relevant [38,39].

This work is supported by "Investissements d'Avenir" LabEx PALM (ANR-10-LABX-0039-PALM). We thank M. Bauer, D. Bernard, P. Carretta, S. Colombo Serra, M. Filibian, Y. Hovav, L. Mazza, and F. Tedoldi for useful discussions. I. Rodriguez Arias and C. Zankoc are acknowledged for the careful reading of the manuscript.

[1] M. Rigol, V. Dunjko, and M. Olshanii, Nature (London) **452**, 854 (2008).
[2] G. Biroli, C. Kollath, and A. M. Läuchli, Phys. Rev. Lett. **105**, 250401 (2010).
[3] D. Basko, I. Aleiner, and B. Altshuler, Ann. Phys. (Amsterdam) **321**, 1126 (2006).
[4] A. Pal and D. A. Huse, Phys. Rev. B **82**, 174411 (2010).
[5] A. Abragam and M. Goldman, Rep. Prog. Phys. **41**, 395 (1978).
[6] J. H. Ardenkjær-Larsen, B. Fridlund, A. Gram, G. Hansson, L. Hansson, M. H. Lerche, R. Servin, M. Thaning, and K. Golman, Proc. Natl. Acad. Sci. U.S.A. **100**, 10158 (2003).
[7] K. Golman, R. in 't Zandt, and M. Thaning, Proc. Natl. Acad. Sci. U.S.A. **103**, 11270 (2006).
[8] L. Lumata, A. K. Jindal, M. E. Merritt, C. R. Malloy, A. D. Sherry, and Z. Kovacs, J. Am. Chem. Soc. **133**, 8673 (2011).
[9] F. Kurdzesau, B. van den Brandt, A. Comment, P. Hautle, S. Jannin, J. van der Klink, and J. Konter, J. Phys. D **41**, 155506 (2008).
[10] B. Provotorov, Sov. Phys. JETP **14**, 1126 (1962).
[11] A. Polkovnikov, K. Sengupta, A. Silva, and M. Vengalattore, Rev. Mod. Phys. **83**, 863 (2011).
[12] Y. Hovav, I. Kaminker, D. Shimon, A. Feintuch, D. Goldfarb, and S. Vega, Phys. Chem. Chem. Phys. **17**, 226 (2015).
[13] Y. Hovav, A. Feintuch, and S. Vega, J. Magn. Reson. **207**, 176 (2010).
[14] A. Karabanov, A. van der Drift, L. J. Edwards, I. Kuprov, and W. Köckenberger, Phys. Chem. Chem. Phys. **14**, 2658 (2012).
[15] Y. Hovav, A. Feintuch, and S. Vega, J. Magn. Reson. **214**, 29 (2012).
[16] H. Jóhannesson, S. Macholl, and J. H. Ardenkjaer-Larsen, J. Magn. Reson. **197**, 167 (2009).
[17] M. Filibian, S. C. Serra, M. Moscardini, A. Rosso, F. Tedoldi, and P. Carretta, Phys. Chem. Chem. Phys. **16**, 27025 (2014).
[18] For the electron spins of trytil radicals at 1.2 K and 3.35 T we have $T_2 \simeq 10^{-6}$ sec versus $T_1 \simeq 1$ sec.
[19] See Supplemental Material at http://link.aps.org/supplemental/10.1103/PhysRevLett.115.080401 for the technical details of our computations. In Sec. I we derive the rates (4a) and (4b) of the master equation. In Sec. II we compute the electron polarization in absence of dipolar interactions. In Sec. III, we derive the simplified master equation for the toy model of Eq. (5). Finally, in Sec. IV we specify the numerical procedures and the parameters used, which includes Refs. [20–23].
[20] M. L. Mehta, *Random Matrices*, 142 (Academic, New York, 2004).
[21] F. Petruccione and H.-P. Breuer, *The Theory of Open Quantum Systems* (Oxford Univ. Press, Oxford, 2002).
[22] P. C. Martin and J. Schwinger, Phys. Rev. **115**, 1342 (1959).
[23] R. Kubo, J. Phys. Soc. Jpn. **12**, 570 (1957).
[24] L. Amico, R. Fazio, A. Osterloh, and V. Vedral, Rev. Mod. Phys. **80**, 517 (2008).
[25] F. Buccheri, A. De Luca, and A. Scardicchio, Phys. Rev. B **84**, 094203 (2011).
[26] A. De Luca and A. Scardicchio, Europhys. Lett. **101**, 37003 (2013).
[27] V. Ros, M. Müller, and A. Scardicchio, Nucl. Phys. **B891**, 420 (2015).
[28] Y. Hovav, A. Feintuch, and S. Vega, Phys. Chem. Chem. Phys. **15**, 188 (2013).
[29] V. Oganesyan and D. A. Huse, Phys. Rev. B **75**, 155111 (2007).
[30] P. Ponte, A. Chandran, Z. Papić, and D. A. Abanin, Ann. Phys. (Amsterdam) **353**, 196 (2015).
[31] G. P. Brandino, A. De Luca, R. M. Konik, and G. Mussardo, Phys. Rev. B **85**, 214435 (2012).
[32] M. Borghini, Phys. Rev. Lett. **20**, 419 (1968).
[33] S. Serra Colombo, A. Rosso, and F. Tedoldi, Phys. Chem. Chem. Phys. **15**, 8416 (2013).
[34] J. H. Ardenkjær-Larsen, S. Macholl, and H. Johannesson, Appl. Magn. Reson. **34**, 509 (2008).
[35] L. Lumata, M. E. Merritt, C. R. Malloy, A. D. Sherry, and Z. Kovacs, J. Phys. Chem. A **116**, 5129 (2012).
[36] S. Colombo Serra, M. Filibian, P. Carretta, A. Rosso, and F. Tedoldi, Phys. Chem. Chem. Phys. **16**, 753 (2014).
[37] V. Atsarkin, Sov. Phys. JETP **31**, 1012 (1970).
[38] V. Bapst, L. Foini, F. Krzakala, G. Semerjian, and F. Zamponi, Phys. Rep. **523**, 127 (2013).
[39] C. R. Laumann, A. Pal, and A. Scardicchio, Phys. Rev. Lett. **113**, 200405 (2014).